

Parametrically Excited Dynamic Bipedal Walking

Fumihiko Asano¹ and Zhi-Wei Luo^{1,2}

¹Bio-Mimetic Control Research Center, Riken, ²Kobe University
Japan

1. Introduction

Human biped locomotion is an ultimate style of biological movement that is a highly evolved function. Biped locomotion by robots is a dream to be attained by the most highly evolved or integrated technology, and research on this has a history of over 30 years.

Many methods of generating gaits have been proposed. There has been a tendency to reduce the complicated dynamics of a walking robot to a simple inverted pendulum (Hemami et al., 1973), and to control its motion according to pre-designed time-dependent trajectories while guaranteeing zero moment point (ZMP) conditions (Vukobratović & Stepanenko, 1972). Although such approaches have successfully been applied to practical applications and nowadays successful biped-himanooids are developed by them, problems on gait performances still remain. Several advanced approaches on the other hand have taken the robot's dynamics into account for generating gaits based on natural dynamics. Miura and Shimoyama studied dynamic bipedal walking without ankle-joint actuation (Miura & Shimoyama, 1984) and they developed robots on stilts whose foot contact occurred at a point. Sano and Furusho accomplished natural dynamic biped walking based on angular momentum using ankle-joint actuation (Sano & Furusho, 1990). Kajita proposed a method of control based on a linear inverted pendulum model with a potential-energy-conserving orbit (Kajita et al., 1992). These approaches utilized the robot's own dynamics effectively but did not investigate the energy-efficiency by introducing performance indices. It was unclear whether or not efficient gaits were generated.

McGeer's passive dynamic walking (PDW) (McGeer, 1990) has provided clues to solve these problems. Passive-dynamic walkers can walk without any actuation on a gentle slope, and they provide an optimal solution to the problem of generating a natural and energy-efficient gait. The objective most expected to be met by PDW is to attain natural, high-speed energy-efficient dynamic bipedal walking on level ground like humans do. However, we need to supply power-input to the robot by driving its joint-actuators to continue stable walking on level ground, and certain methods of supplying power must be introduced.

Ankle-joint torque is mathematically very important for effectively propelling the robot's center of mass (CoM) in the walking direction, and it is thus required relatively more often than other joint torques. However, to exert ankle-joint torque on a passive-dynamic walker, we need to add feet and this creates the ZMP constraint problem. We clarified that there is a trade-off between optimal gait and ZMP conditions through parametric studies, and

Source: Bioinspiration and Robotics: Walking and Climbing Robots, Book edited by Maki K. Habib
ISBN 978-3-902613-15-8, pp. 544, I-Tech, Vienna, Austria, EU, September 2007

concluded that generating an energy-efficient and high-speed dynamic biped gait is difficult using approaches based on ankle-joint actuation (Asano et al., 2004). Utilizing the torso can be considered to solve this problem and we should use the joint torques between the torso, stance, and swing-leg. Another difficulty, however, then arises as to how to drive the legs while stably balancing the torso. Kinugasa investigated this problem by using virtual gravity approach (Kinugasa, 2002).

A question then arises as to how to generate energy-efficient and high-speed dynamic biped locomotion without taking ZMP conditions into account or controlling the torso balance. This question further leads us to conclusion that if the leg itself has a mechanism to increase mechanical energy, these difficulties can be overcome. The answer can be found in the principle of parametric excitation. Minakata and Tadakuma experimentally demonstrated that level dynamic walking could be accomplished by pumping the leg mass (Minakata & Tadakuma, 2002). This suggests that a dynamic biped gait can be generated without any rotational actuation, merely by pumping the motion of the leg. This mechanism can be understood as the effect of parametric excitation from the mechanical energy point of view, and we investigate the detailed mechanical principles underlying it.

Fig. 1 has a model of a swing-person system; point mass m has a variable-length pendulum whose mass and inertia moment can be neglected. Here, θ [rad] is the anticlockwise angle of deviation for the pendulum from the vertical and $g = 9.81$ [m/s²] is the gravity acceleration. Let

$$l_0 \leq l \leq l_1, \quad (1)$$

$$-\pi \leq \theta \leq \pi, \quad (2)$$

where l_0 and l_1 [m] are constant and $l_1 \geq l_0$. The proof for optimal control to increase mechanical energy can be described as follows. Let L [kg·m²/s] be the angular momentum of the system, which is given by

$$L = ml^2 \dot{\theta}, \quad (3)$$

and its time derivative satisfies the relation

$$\dot{L} = -mgl \sin \theta. \quad (4)$$

According to this, the optimal control to increase mechanical energy is

$$l = \begin{cases} l_1 & (\theta \leq 0) \\ l_0 & (\theta > 0) \end{cases}. \quad (5)$$

The mechanical energy is restored and maximized as well as the angular momentum by moving the mass from A to E as shown in Fig. 1, and restored value ΔE [J] yields

$$\Delta E = mg(l_1 - l_0)(1 - \cos \theta_0), \quad (6)$$

where θ_0 [rad] is the deviation angle when $\dot{\theta} = 0$ (at D and E positions). Lavrovskii and Formalskii provide further details (Lavrovskii & Formalskii, 1993). In the following, we discuss how we applied this pumping mechanism to controlling the swing-leg of a planar telescopic-legged biped robot.

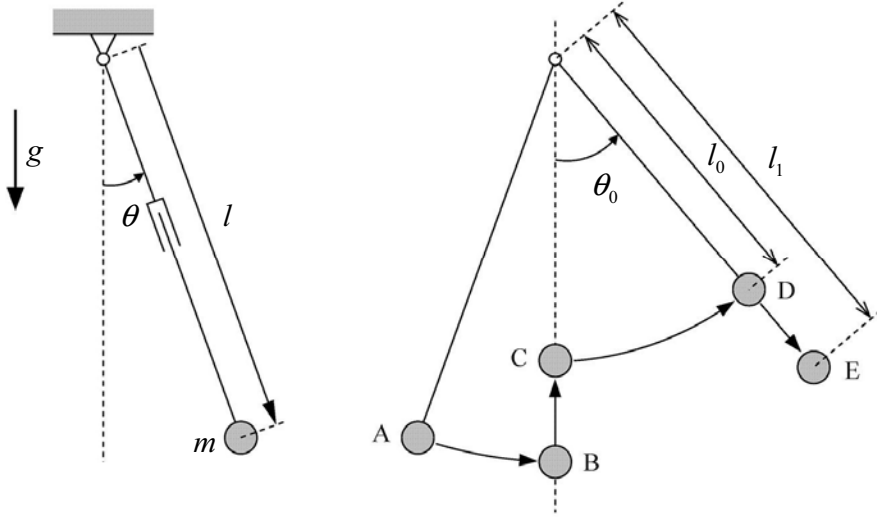


Figure 1. Swing-person system and optimal control to increase mechanical energy

2. Modelling Planar Telescopic-legged Biped

This section describes the mathematical model for the simplest planar biped robot with telescopic legs.

2.1 Dynamic equation

In this chapter, we deal with a planar biped robot with telescopic legs as shown in Fig. 2. We assumed that the robot did not have rotational actuators at the hip or ankle joints, and only had telescopic actuators on the legs. By moving the swing-leg's mass in the leg direction following our proposed method, the robot system can increase the mechanical energy based on how effective parametric excitation is. We assumed that the stance leg's actuator would be mechanically locked during the stance phase maintaining the length $b_1 = b$ where b is constant. The length of the lower parts, a_1 and a_2 , is equal to constant a . The swing-leg length, b_2 , was also adjusted to the desired values before heel-strike impact. The robot can then be modeled as a 3-DOF system whose generalized coordinate vector is $\mathbf{q} = [\theta_1 \quad \theta_2 \quad b_2]^T$, as shown in Fig. 2. The dynamic equation is given by

$$\mathbf{M}(\mathbf{q})\ddot{\mathbf{q}} + \mathbf{h}(\mathbf{q}, \dot{\mathbf{q}}) = \mathbf{S}\mathbf{u} = \begin{bmatrix} 0 \\ 0 \\ 1 \end{bmatrix} u \quad (7)$$

where $\mathbf{M}(\mathbf{q}) \in \mathbf{R}^{3 \times 3}$ is the inertia matrix and $\mathbf{h}(\mathbf{q}, \dot{\mathbf{q}}) \in \mathbf{R}^3$ is the vector for Coriolis, centrifugal, and gravity forces. The u is the control input for the telescopic actuator on the swing leg.

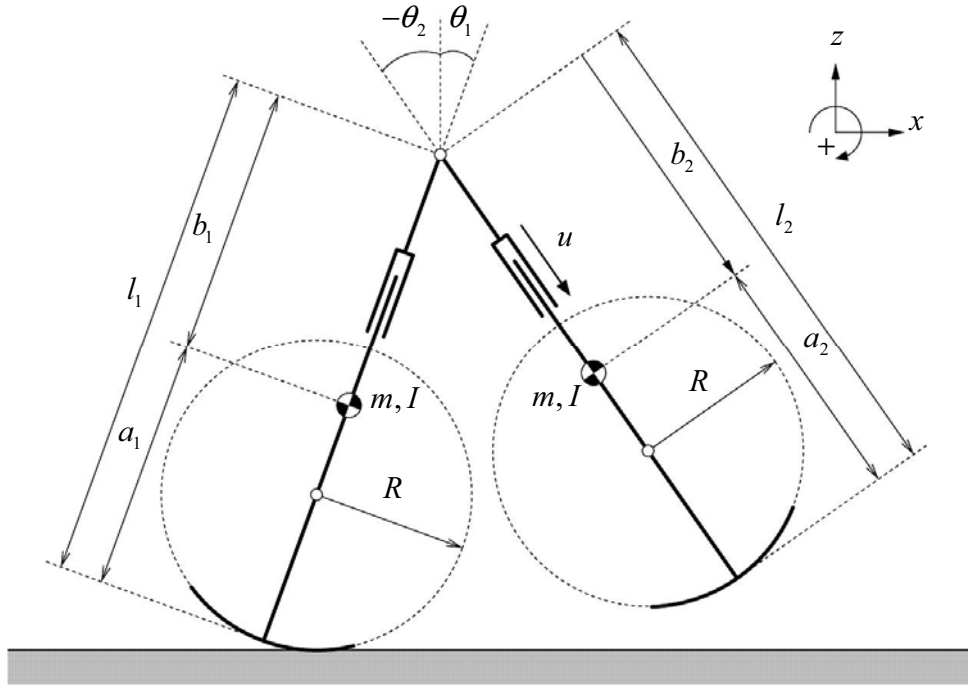


Figure 2. Model of planar telescopic legged biped with semicircular feet

Several past researchers have been considered the telescopic-leg mechanism in PDW. Although van der Linde introduced it as a compliance mechanism (van der Linde, 1998) and Osuka and Saruta adopted it to avoid foot-scuffing during the stance phase (Osuka & Saruta, 2000), its dynamics and effect on restoring mechanical energy have thus far not been investigated.

2.2 Transition equation

The positional state variables can be reset very easily. Assuming that the pumping of the swing-leg has been controlled before heel-strike impact, i.e., the swing leg is as long as the stance leg (nominal length), the robot is symmetrical with respect to the z -axis, as shown in Fig. 3. The positional vector, \mathbf{q} , should be then reset as

$$\mathbf{q}^+ = \begin{bmatrix} 0 & 1 & 0 \\ 1 & 0 & 0 \\ 0 & 0 & 1 \end{bmatrix} \mathbf{q}^-. \quad (8)$$

The velocities, on the other hand, are reset according to the following algorithms by introducing the extended generalized coordinate vector, $\bar{\mathbf{q}} \in \mathbf{R}^6$. The heel-strike collision model can be modeled as

$$\bar{\mathbf{M}}(\bar{\mathbf{q}})\dot{\bar{\mathbf{q}}}^+ = \bar{\mathbf{M}}(\bar{\mathbf{q}})\dot{\bar{\mathbf{q}}}^- - \mathbf{J}_I(\bar{\mathbf{q}})^T \boldsymbol{\lambda}_I, \quad (9)$$

$$\mathbf{J}_I(\bar{\mathbf{q}})\dot{\bar{\mathbf{q}}}^+ = \mathbf{0}_{4 \times 1}, \quad (10)$$

where $\mathbf{J}_I(\bar{\mathbf{q}}) \in \mathbf{R}^{4 \times 6}$ is the Jacobian matrix derived following the geometric condition at impact, $\boldsymbol{\lambda}_I \in \mathbf{R}^4$ is Lagrange's undetermined multiplier vector within the context of impulsive force, and Eq. (10) represents the post-impact velocity constraint conditions. The generalized coordinate vector in this case is defined as

$$\bar{\mathbf{q}} = \begin{bmatrix} \bar{\mathbf{q}}_1 \\ \bar{\mathbf{q}}_2 \end{bmatrix}, \quad \bar{\mathbf{q}}_i = \begin{bmatrix} x_i \\ z_i \\ \theta_i \end{bmatrix}. \quad (11)$$

The inertia matrix, $\bar{\mathbf{M}}(\bar{\mathbf{q}}) \in \mathbf{R}^{6 \times 6}$, is derived according to $\bar{\mathbf{q}}$, and detailed as

$$\bar{\mathbf{M}}(\bar{\mathbf{q}}) = \begin{bmatrix} \bar{\mathbf{M}}_1(\bar{\mathbf{q}}_1) & \mathbf{0}_{3 \times 3} \\ \mathbf{0}_{3 \times 3} & \bar{\mathbf{M}}_2(\bar{\mathbf{q}}_2) \end{bmatrix}, \quad (12)$$

where the matrix, $\bar{\mathbf{M}}_i(\bar{\mathbf{q}}_i) \in \mathbf{R}^{3 \times 3}$, is the inertia matrix for leg i . Note $\bar{\mathbf{q}} = \bar{\mathbf{q}}^+ = \bar{\mathbf{q}}^-$ in Eq. (9), and impulsive force vector $\boldsymbol{\lambda}_I$ in Eq. (9) can be derived as

$$\boldsymbol{\lambda}_I = \mathbf{X}_I^{-1} \mathbf{J}_I \dot{\bar{\mathbf{q}}}^-, \quad \mathbf{X}_I = \mathbf{J}_I \bar{\mathbf{M}}^{-1} \mathbf{J}_I^T. \quad (13)$$

By substituting Eq. (13) into (9), we obtain

$$\dot{\bar{\mathbf{q}}}^+ = (\mathbf{I}_6 - \bar{\mathbf{M}}^{-1} \mathbf{J}_I^T \mathbf{X}_I^{-1} \mathbf{J}_I) \dot{\bar{\mathbf{q}}}^-. \quad (14)$$

Semicircular feet have shock absorbing effect; they decrease mechanical energy dissipation caused by the impact of heel-strike. The authors theoretically investigated the detailed mechanism and clarified that there is a condition to decrease mechanical energy dissipation to zero when the foot radius is equal to the leg length (Asano & Luo, 2007). By utilizing this

effect, the robot can effectively promote parametric excitation and increase the walking speed effectively.

2.3 Mechanical energy

The total mechanical energy, E [J], is defined by the sum of kinetic and potential energy as

$$E(\mathbf{q}, \dot{\mathbf{q}}) = \frac{1}{2} \dot{\mathbf{q}}^T \mathbf{M}(\mathbf{q}) \dot{\mathbf{q}} + P(\mathbf{q}), \quad (15)$$

and its time derivative satisfies the relation

$$\dot{E} = \dot{\mathbf{q}}^T \mathbf{S} \mathbf{u} = \dot{b}_2 u. \quad (16)$$

It remains constant with zero-input, or passive dynamic walking on a gentle slope. It should be steadily increased during the stance phase on level ground to restore the lost energy by every heel-strike collisions.

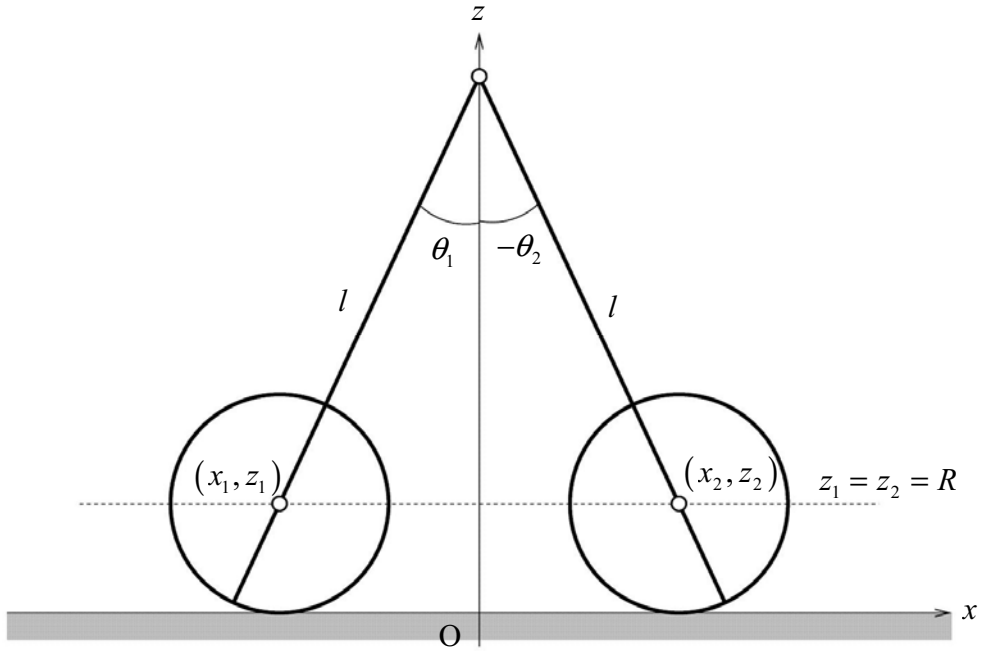


Figure 3. Configuration at instant of heel-strike

3. Parametrically Excited Dynamic Bipedal Walking

This section describes a simple law to control telescopic leg actuation and investigates a typical dynamic gait produced by the effect of parametric excitation.

3.1 Control law

A level gait can be generated by simply controlling pumping to the swing-leg. We propose output following control in this chapter to reproduce the parametric excitation mechanism in Fig. 1 by expanding and contracting the swing-leg length. We chose the telescopic length of the swing-leg, $b_2 = \mathbf{S}^T \mathbf{q}$, as the system's output, and its second order derivative yields

$$\ddot{b}_2 = \mathbf{S}^T \mathbf{M}(\mathbf{q})^{-1} \mathbf{S} u - \mathbf{S}^T \mathbf{M}(\mathbf{q})^{-1} \mathbf{h}(\mathbf{q}, \dot{\mathbf{q}}). \quad (17)$$

Let $b_{2d}(t)$ be the time-dependent trajectory for b_2 , and the control input that exactly achieves $b_2 \equiv b_{2d}(t)$ can be determined as

$$\mathbf{u} = \left(\mathbf{S}^T \mathbf{M}(\mathbf{q})^{-1} \mathbf{S} \right)^{-1} \left(\ddot{b}_{2d} + \mathbf{S}^T \mathbf{M}(\mathbf{q})^{-1} \mathbf{h}(\mathbf{q}, \dot{\mathbf{q}}) \right). \quad (18)$$

We give the control input in Eq. (18) as a continuous-time signal to enable the exact gait to be evaluated. Considering smooth pumping motion, we intuitively introduced a time-dependent trajectory, $b_{2d}(t)$, to enable telescopic leg motion:

$$b_{2d}(t) = \begin{cases} b - A \sin^3 \left(\frac{\pi}{T_{\text{set}}} t \right) & (t \leq T_{\text{set}}), \\ b & (t > T_{\text{set}}), \end{cases} \quad (19)$$

where T_{set} [s] is the desired settling-time, and where we assumed that T_{set} would occur before heel-strike collisions. In other words, let T [s] be the steady-step period, condition $T \geq T_{\text{set}}$ should always hold. We called this the settling-time condition. Since $\ddot{b}_{2d}(T_{\text{set}})$ is not differentiable but continuous here, the control input, \mathbf{u} , also becomes continuous.

3.2 Numerical simulations

Fig. 4 shows the simulation results for parametrically excited dynamic bipedal walking where $A = 0.08$ [m] and $T_{\text{set}} = 0.55$ [s]. The same physical parameters were chosen as in Table 1. Fig. 5 shows one cycle of motion of the walking pattern. We can see from the results that a stable limit cycle is generated by the effect of the proposed method. We can see from Figs. 4 (b) and (c) that the leg length is successfully controlled and settled to the desired length b [m] before all heel-strike collisions whereas the mechanical energy is restored by the effect of parametric excitation. Stable dynamic biped level locomotion can be easily achieved without taking the ZMP condition into account since this robot does not use (or require) ankle-joint torque. The ZMP in this case is identical to the contact point of the sole with the ground, and travels forward monotonically from the heel to the tiptoe assuming that condition $\dot{\theta}_1 > 0$ holds. This property appears human-like.

Note that, as seen in (c), the mechanical energy is not restored monotonically but lost by expanding the swing leg. It is necessary to monotonically restore mechanical energy to

obtain maximum efficiency (Asano et al., 2005), and how to improve this will be investigated in the next section.

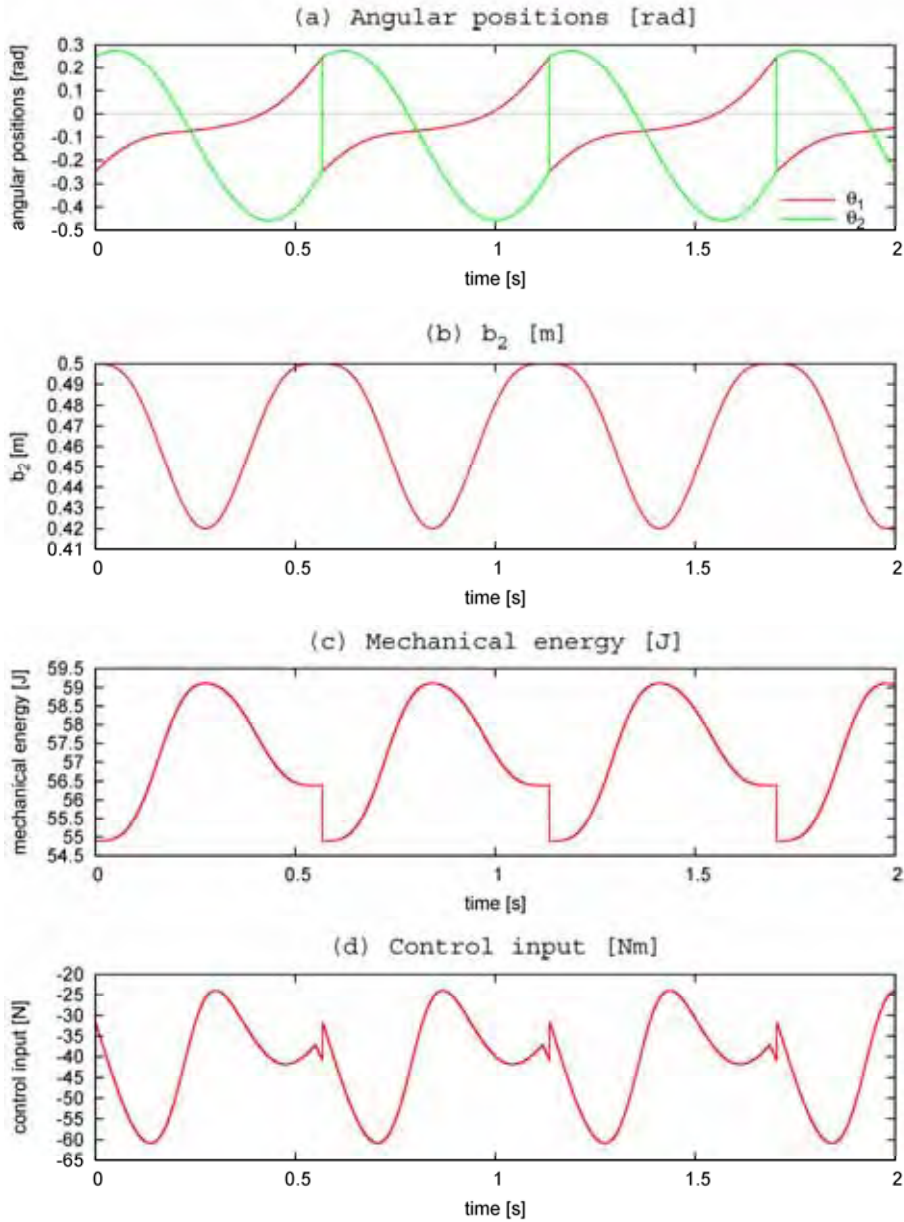


Figure 4. Simulation results for parametrically excited dynamic bipedal walking where $A = 0.08$ [m] and $T_{\text{set}} = 0.55$ [s]

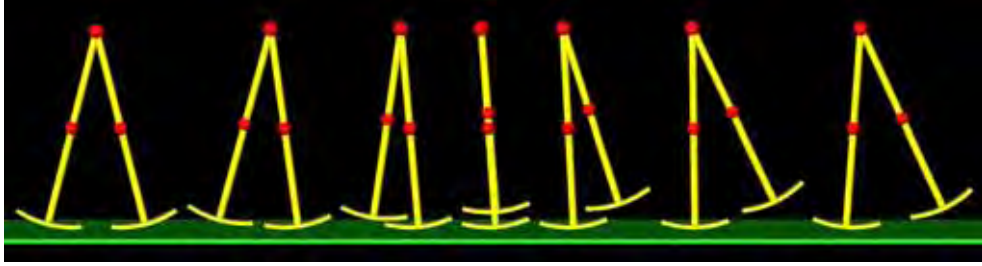


Figure 5. One cycle of motion for parametrically excited dynamic bipedal walking in Fig. 4

m		5.0	kg
I		0.1	$\text{kg} \cdot \text{m}^2$
l	$= a + b$	1.0	m
a		0.5	m
b		0.5	m
R		0.5	m

Table 1. Physical parameters of telescopic-legged biped robot in Fig. 2

4. Improvements in Energy-efficiency Using Elastic Element

Since the pumping motion of swing leg causes energy loss, as mentioned in Section 3, it leads to inefficient walking. This section therefore investigates improved energy-efficiency achieved by using an elastic element and adjusting its mechanical impedances.

4.1 Model with elastic elements

Telescopic leg actuation requires very large torque to raise the entire leg mass and this causes inefficient dynamic walking. The utilization of elastic elements should be considered to solve this problem. This section introduces a model with elastic elements and we analyze its effectiveness through numerical simulations.

Fig. 6 outlines a biped model with elastic elements where $k > 0$ is the elastic coefficient and b_0 is the nominal length. Its dynamic equation during the swing phase is given by

$$M(q)\ddot{q} + h(q, \dot{q}) = Su - \frac{\partial Q}{\partial q^T}, \quad (20)$$

where Q is the elastic energy defined as

$$Q = \frac{1}{2}k(b_2 - b_0)^2. \quad (21)$$

The other terms except for the elastic effect are the same as those in Eq. (7).

We here redefine the total mechanical energy including the elastic energy, Q , as

$$E(\mathbf{q}, \dot{\mathbf{q}}) = \frac{1}{2} \dot{\mathbf{q}}^T \mathbf{M}(\mathbf{q}) \dot{\mathbf{q}} + P(\mathbf{q}) + Q(\mathbf{q}), \quad (22)$$

and its time-derivative yields

$$\dot{E} = \dot{b}_2 u. \quad (23)$$

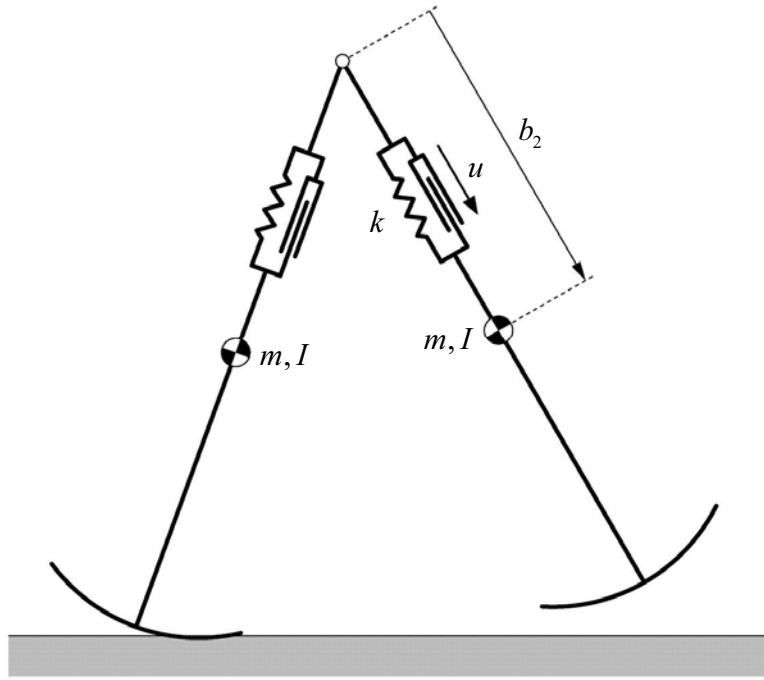


Figure 6. Model of planar telescopic legged biped with elastic elements

4.2 Performance indices

Let us introduce criterion functions before performing numerical analysis. Let T [s] be the steady step period. For simplicity, every post-impact (or start) time has been denoted in the following as $t = 0^+$ and every pre-impact time of the next heel-strike as T^- by resetting the absolute time at every transition instant. Thus T^+ means the same as 0^+ . The average walking speed v [m/s] is then defined as

$$v = \frac{\Delta x_G}{T}, \quad (24)$$

where x_G [m] is the x -position at the robot's center of mass and $\Delta x_G \triangleq x_G(T^-) - x_G(0^+)$ [m] is the change in one step. The average input power is also defined as

$$p = \frac{1}{T} \int_{0^+}^{T^-} |\dot{b}_2 u| dt. \quad (25)$$

Energy-efficiency is then evaluated by specific resistance p / Mgv [-], which means the expenditure of energy per unit mass and per unit length, and this is a dimension-less quantity. The main question of how to attain energy-efficient biped locomotion rests on how to increase walking speed v while keeping p small.

4.3 Efficiency analysis

The control input, u , to exactly achieve $b_2 \equiv b_{2d}$ in this case is determined to cancel out the elastic effect in Eq. (20) as

$$u = \left(\mathbf{S}^T \mathbf{M}(\mathbf{q})^{-1} \mathbf{S} \right)^{-1} \left(\ddot{b}_{2d} + \mathbf{S}^T \mathbf{M}(\mathbf{q})^{-1} \left(\mathbf{h}(\mathbf{q}, \dot{\mathbf{q}}) + \frac{\partial Q}{\partial \mathbf{q}^T} \right) \right). \quad (26)$$

This does not change walking motion regardless of the elastic element's mechanical impedances. Only the actuator's burden is adjusted. The maximum energy-efficiency condition is then found in the combination of k and b_0 that minimize the average input power, p . The following relation holds for the definite integral of the absolute function to calculate p ,

$$p \geq \frac{1}{T} \int_{0^+}^{T^-} \dot{b}_2 u dt = \frac{1}{T} \int_{0^+}^{T^-} \dot{E} dt = \frac{\Delta E}{T}, \quad (27)$$

where $\Delta E \triangleq E(T^-) - E(0^+)$ [J] is the restored mechanical energy in one cycle, and it should be positive if a stable gait is generated. Therefore, following Eqs. (24) and (27), we can obtain the relation

$$\frac{p}{Mgv} \geq \frac{\Delta E}{Mg \Delta x_G}. \quad (28)$$

Where $M \triangleq 2m$ [kg] is the robot's total mass. Here note that the equality holds in Eq. (27) if and only if $\dot{E} = \dot{b}_2 u \geq 0$. This means that the monotonic restoration of mechanical energy by control input is the necessary condition for maximum efficiency (Asano et al., 2005).

Fig. 7 shows the specific resistance with respect to k and b_0 with its contours. There is an optimal combination of k and b_0 in the valley of the 3-D plot, and the specific resistance is kept quite small at less than 0.04, which is much smaller than that of previous results (Gregorio et al., 1997). The gait obtained with optimal mechanical impedances is much faster than that with virtual passive dynamic walking at the same value for specific resistance. As previously mentioned, elastic effect increases the energy-efficiency without destroying the generated high-speed parametrically-excited gait. In such cases, total mechanical energy including elastic energy defined by Eq. (22) almost monotonically increases during a cycle, i.e., maximum efficiency condition is achieved. The optimal mechanical impedances, however, must be found by conducting numerical simulations.

The edges of the 3-D plot in Fig. 7 are lines where $k = 0$ and $b_0 = 0.46$ with the same value. The specific resistance where $k = 0$ is of course kept constant regardless of b_0 , i.e., the value without any power assist. On the other hand, $b_0 = 0.46$ [m] yields the same efficiency as in the case of $k = 0$ regardless of k . This can be explained as follows. Eq. (26) can be expressed as

$$u = u_0 + k(b_2 - b_0), \quad (29)$$

where u_0 is the same as u in Eq. (18). The sign of u is always negative when $b_0 = b - \frac{A}{2}$, thus that of $\dot{E} = \dot{b}_2 u$ is equivalent to that of $-\dot{b}_2$. The input power integral can then be divided as follows.

$$\begin{aligned} \int_{0^+}^{T^-} |\dot{b}_2 u| dt &= \int_{0^+}^{T_{\text{set}}/2} \dot{b}_2 u dt - \int_{T_{\text{set}}/2}^{T_{\text{set}}} \dot{b}_2 u dt \\ &= \int_{0^+}^{T_{\text{set}}/2} \dot{b}_2 (u_0 + k(b_2 - b_0)) dt - \int_{T_{\text{set}}/2}^{T_{\text{set}}} \dot{b}_2 (u_0 + k(b_2 - b_0)) dt. \end{aligned} \quad (30)$$

Here the following relations hold.

$$\begin{aligned} \int_{0^+}^{T_{\text{set}}/2} \dot{b}_2 k (b_2 - b_0) dt &= \left[\frac{1}{2} k (b_2 - b_0)^2 \right]_{b_2=b_0+\frac{A}{2}}^{b_2=b_0-\frac{A}{2}} = 0 \\ \int_{T_{\text{set}}/2}^{T_{\text{set}}} \dot{b}_2 k (b_2 - b_0) dt &= \left[\frac{1}{2} k (b_2 - b_0)^2 \right]_{b_2=b_0-\frac{A}{2}}^{b_2=b_0+\frac{A}{2}} = 0 \end{aligned} \quad (31)$$

Therefore, we can see that in this case the term for elastic effect does not influence the energy-efficiency at all. We should choose a b_0 of less than $b - \frac{A}{2}$ to ensure efficiency is improved.

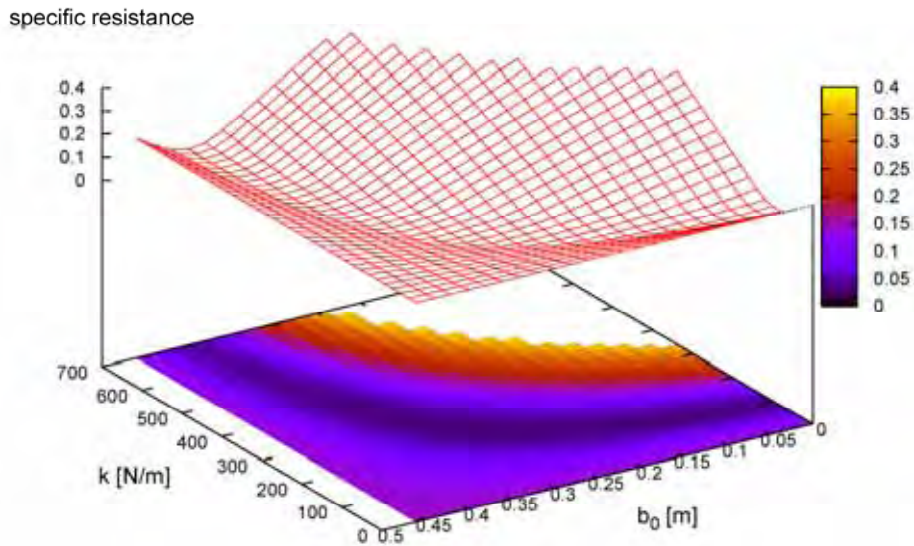


Figure 7. Specific resistance with respect to elastic coefficient and nominal leg length

5. Conclusion

This chapter described a novel method of generating a biped gait based on the principle of parametric excitation. We confirmed the validity of swing-leg actuation through numerical simulations. A high-speed and energy-efficient gait was easily accomplished by pumping the swing-leg mass. We confirmed that energy-efficiency can be improved by using elastic elements without changing the walking pattern. It is possible to achieve a minimum class of specific resistance by optimally adjusting mechanical impedances to satisfy maximum efficiency condition.

The greatest contribution of our study was achieving energy-efficient and high-speed dynamic biped locomotion without having to take ZMP conditions into account. We hope that our approach will provide new concepts for the introduction of *ZMP-free biped robots*.

6. References

- Asano, F., Luo, Z.W. & Yamakita, M. (2005). Biped gait generation and control based on a unified property of passive dynamic walking, *IEEE Transactions on Robotics*, Vol.21, No.4, pp.754--762, Aug. 2005.
- Asano, F., Luo, Z.W. & Yamakita, M. (2004). Unification of dynamic gait generation methods via variable virtual gravity and its control performance analysis, *Proc. of the IEEE/RSJ Int. Conf. on Intelligent Robots and Systems (IROS)*, pp.3865--3870, Oct. 2004.
- Asano, F. & Luo, Z.W. (2007). The effect of semicircular feet on energy dissipation by heel-strike in dynamic biped locomotion, *Proc. of the IEEE Int. Conf. on Robotics and Automation (ICRA)*, pp. 3976--3981, Apr. 2007.
- Gregorio, P., Ahmadi, M. & Buehler, M. (1997). Design, control, and energetics of an electrically actuated legged robot, *IEEE Trans. on Systems, Man and Cybernetics--Part B: Cybernetics*, Vol.27, No.4, pp.626--634, Aug. 1997.
- Hemami, H., Weimer, F.C. & Koozekanani, S.H. (1973). Some aspects of the inverted pendulum problem for modeling of locomotion systems, *IEEE Trans. on Automatic Control*, Vol.18, No.6, pp.658--661, Dec. 1973.
- Kajita, S., Kobayashi, A. & Yamaura, T. (1992). Dynamic walking control of a biped robot along a potential energy conserving orbit, *IEEE Trans. on Robotics and Automation*, Vol.8, No.4, pp.431--438, Aug. 1992.
- Kinugasa, T. (2002). Biped walking of Emu based on passive dynamic walking mechanism, *Proc. of the ICASE/SICE Workshop --Intelligent Control and Systems*, pp.304--309, Oct. 2002.
- McGeer, T. (1990). Passive dynamic walking, *Int. J. of Robotics Research*, Vol.9, No.2, pp.62--82, Apr. 1990.
- Miura, H. & Shimoyama, I. (1984). Dynamic walk of a biped, *Int. J. of Robotics Research*, Vol.3, No.2, pp.60--74, Apr. 1984.
- Lavrovskii E.K. & Formalskii, A.M. (1993). Optimal control of the pumping and damping of a swing, *J. of Applied Mathematics and Mechanics*, Vol.57, No.2, pp.311--320, 1993.
- van der Linde, R.Q. (1998). Active leg compliance for passive walking, *Proc. of the IEEE Int. Conf. on Robotics and Automation (ICRA)*, Vol.3, pp.2339--2345, May 1998.
- Minakata, H. & Tadakuma, S. (2002). An experimental study of passive dynamic walking with non-rotate knee joint biped, *Proc. of the ICASE/SICE Workshop --Intelligent Control and Systems*, pp.298--303, Oct. 2002.
- Osuka K. & Saruta, Y. (2000). Development and control of new legged robot Quartet III -- From active walking to passive walking, *Proc. of the IEEE/RSJ Int. Conf. on Intelligent Robots and Systems (IROS)*, Vol.2, pp.991--995, Oct. 2000.
- Sano, A. & Furusho, J. (1990). Realization of natural dynamic walking using the angular momentum information, *Proc. of the IEEE Int. Conf. on Robotics and Automation (ICRA)*, Vol.3, pp.1476--1481, May 1990.